

Ultralight and highly compressible coal oxide-modified graphene aerogels for organic solvents absorption and light-to-heat conversion

Shengchao Hou, Yan Lv, Xueyan Wu, Jixi Guo*, Qingqing Sun, Luxiang Wang,

Dianzeng Jia*

Key Laboratory of Energy Materials Chemistry, Ministry of Education; Key Laboratory of Advanced Functional Materials, Autonomous Region; Institute of Applied Chemistry, Xinjiang University, Urumqi, 830046, Xinjiang P. R. China.

Email: jxguo1012@163.com; jdz@xju.edu.cn; Fax: +86-991-8588883; Tel: +86-991-

8583083.

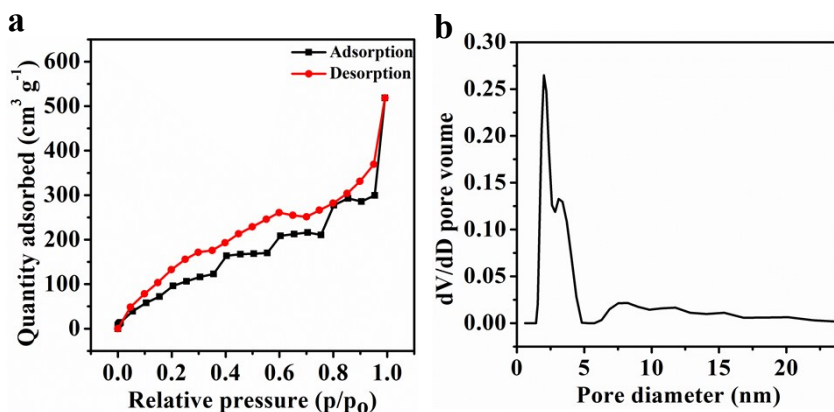


Figure S1 (a) The nitrogen adsorption and desorption isotherms in Brunauer-Emmett-Teller (BET) measurement, (b) The pore size distribution of MGC.

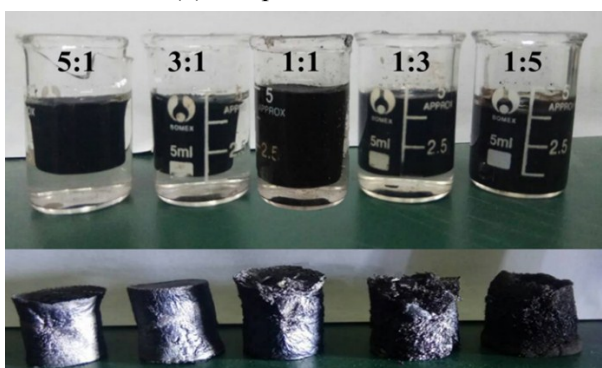


Figure S2. The variation in appearance of hydrogels and aerogels with different mass ratios (5:1, 3:1, 1:1, 1:3 and 1:5, respectively; dopamine hydrochloride=6 mg) of GO and CO with the precursor concentration of 4 mg cm^{-3} .

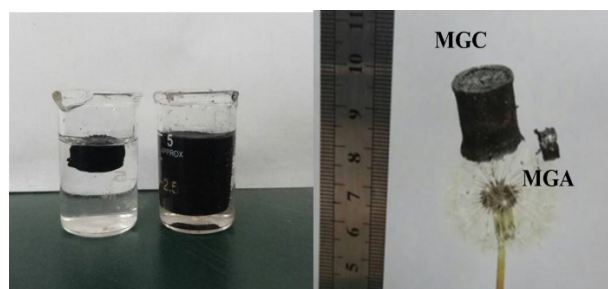


Figure S3. The hydrogel appearance of GA and GC with the precursor concentration of 4 mg cm^{-3} and photograph of ultralight MGA and MGC samples on dandelion

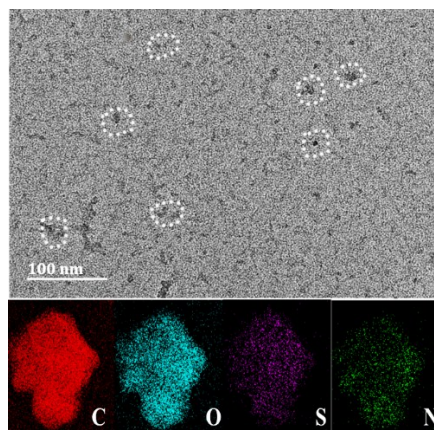


Figure S4. TEM images of coal oxide and corresponding elemental mapping.

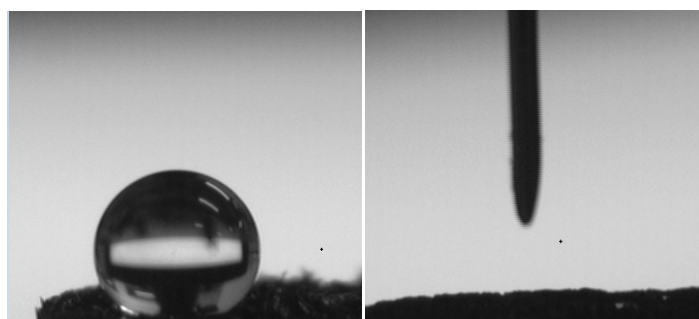


Figure S5. Optical image of water droplet and dichloromethane on the surface of the MGC in contact angle measurement.

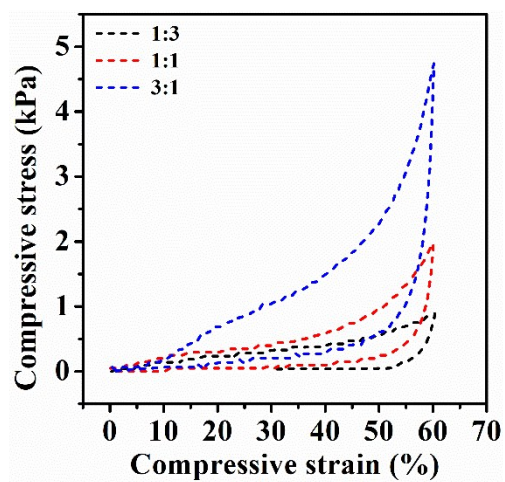


Figure S6. Cyclic compression curves of modified aerogels with different CO concentrations.

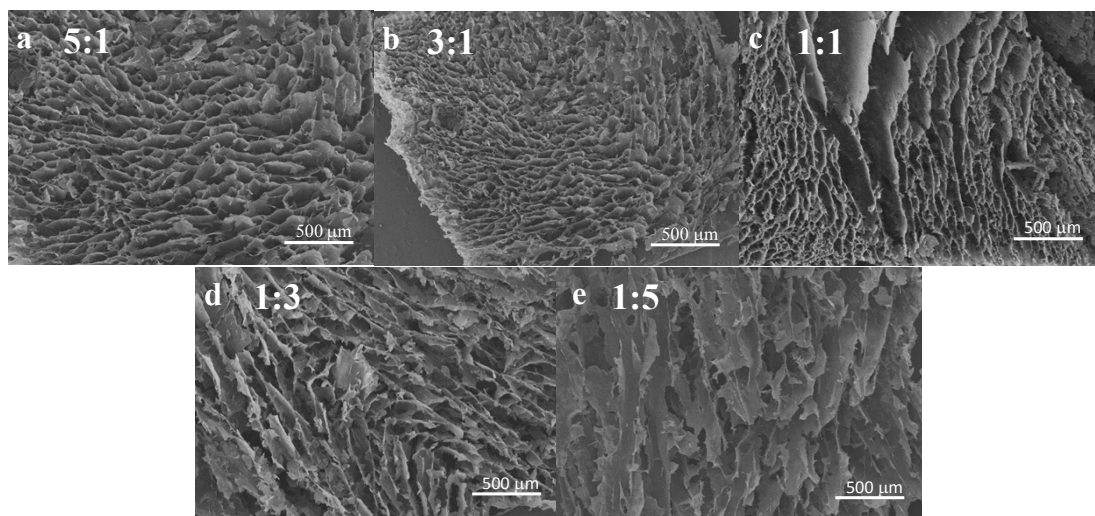


Figure S7. The SEM images of the composite aerogels with different feeding ratio of GO and CO, (a) 5:1, (b) 3:1, (c) 1:1, (d) 1:3 and (e) 1:5.

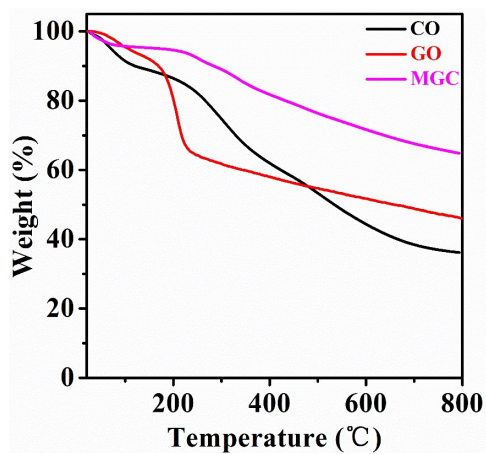


Figure S8. TGA curve of MGC performed under an N₂ atmosphere with heating rate of 10 °C min⁻¹.

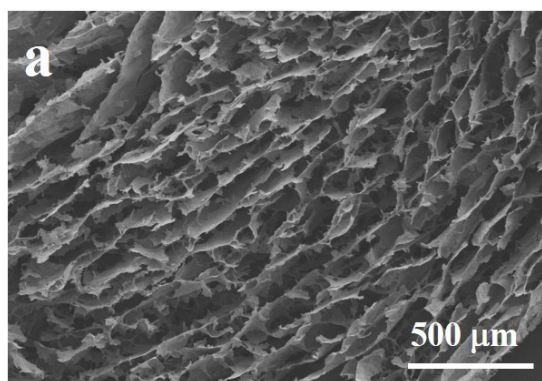


Figure S9. SEM images of MGC after oil recycling: (a) combustion method.

Table S1. Atom percentage of GC and MGC from XPS survey scans.

	C (%)	O (%)	Si (%)	N (%)
GC	57.86	38.97	0	3.17
MGC	82.56	11.33	5.28	0.83

Table S2. The proportion of different bonds with Gauss fitted for XPS curves.

	GC		MGC	
	position	%	position	%
C-C	284.88	64.9	284.78	91.6
C-O	286.28	24.8	286.28	7.5
C=O	288.68	12.3	288.68	0.9

Table S3. Comparison of various graphene-based absorbent materials.

Sorbents	Absorbates	Capacity (g g ⁻¹)	Ref.
Graphene sponges	Oils and organic solvents	20–86	42
Graphene aerogels	Organic liquids	120–200	43
Magnetic graphene foam	Oil and organic solvents	10–27	44
Peanut hull/graphene aerogel	Oil and organic solvents	32–79	8
Nanofiber/graphene aerogel	Oils absorption	120–286	45
Graphene/ cellulose aerogel	Organic solvents	44–265	46
Carbon nanotubes/graphene aerogel	Organic compounds	322±8.3	3

Table S4. Comparison of various bioass-based absorbent materials.

Sorbents	Absorbates	Capacity (g g ⁻¹)	Ref.
Coal-based fiber	Organic matter	0.07	12
Melamine/lignin sponges	Oil	98–217	47
Lignin-based xerogel	Oils and organic solvents	19–47	48
Cellulose nanofibrils aerogel	Oil	88–143	49
Twisted carbon fibers	Oils and organic solvents	50–190	11
Bamboo-based aerogel	Oils and organic solvents	30–129	50
sodium alginate foams	Oils and organic solvents	73–187	51
Graphene/coal oxide aerogels	Oils and organic solvents	93–196	This work
Carbonated graphene/coal oxide aerogels	Oils and organic solvents	170–387	This work

